



1 **Global detection of rainfall triggered landslide clusters**

2 Susanne A. Benz^{1,2}, Philipp Blum¹

3 ¹ Karlsruhe Institute of Technology (KIT), Institute of Applied Geosciences (AGW), Karlsruhe, Germany

4 ² University of California San Diego (UCSD), School of Global Policy and Strategy (GPS), La Jolla, CA, USA

5 *Correspondence to:* Philipp Blum (blum@kit.edu) and Susanne A. Benz (sabenz@ucsd.edu)

6 **Abstract**

7 An increasing awareness of the cost of landslides on the global economy and of the associated loss
8 of human life, has led to the development of various global landslide databases. However, these
9 databases typically report landslide events instead of individual landslides, i.e. a group of landslides
10 with a common trigger and reported by media, citizens and/or government officials as a single unit.
11 The latter results in significant cataloging and reporting biases. To counteract this biases, this study
12 aims to identify clusters of landslide events that were triggered by the same rainfall event. Here the
13 developed algorithm is applied to the Global Landslide Catalog (GLC) maintained by NASA. The
14 results show that more than 40 % of all landslide events are connected to at least one other event,
15 and that 14 % of all studied landslide events are actually part of a landslide cluster consisting of at
16 least 10 events. However, in a more regional analysis this number ranges from 30 % for the West
17 Coast of North America to 3 % in the Himalaya Region. The cluster with most landslide events in
18 a day is located in Rio de Janeiro, Brazil, with 108 events on 6th April 2010. In contrast, the longest
19 running cluster was observed on the West Coast of North America with 132 events occurring in an
20 area of over 120,000 km² during 24 days in December 2015. Our study intends to enhance our
21 understanding of landslide clustering and thus will assist in the development of improved,
22 internationally streamlined mitigation strategies for rainfall related landslide clusters.



23 **Keywords:** Landslide events; Database; Extreme weather; Rainfall induced; Early warning
24 systems;

25 **1. Introduction**

26 The fatal and catastrophic nature of landslides has led to the development and maintenance of
27 various global databases, such as the NASA Global Landslide Catalogue (GLC; e.g. Kirschbaum
28 et al. 2015) and recently the Global Fatal Landslide Database (GFLD) by Froude & Petley (2018).
29 Typically, these databases have a distinct focus. For example, the Global Landslide Catalogue
30 (GLC) operated by NASA focuses on rainfall triggered landslides (Kirschbaum et al., 2010, 2015),
31 whereas the Global Fatal Landslide Database records fatal landslides (Froude and Petley, 2018;
32 Petley, 2012). Through these databases we are able to provide first estimates on the number of
33 recorded fatalities, which were > 55,000 between 2004 and 2016 (Froude and Petley, 2018) and
34 map near real-time risk for landslides almost on a global scale (Kirschbaum and Stanley, 2018).
35 Still, while they play a key role in understanding the effects of landslides on our society, it is
36 important to note that they are primarily based on news and government reports. These databases
37 therefore do not count landslides, but landslide events, which contain either a single or a multitude
38 of landslides within an area that are assumed to be triggered by the same event (Malamud et al.,
39 2004). The exact number of slope failures in each event is often unknown and depends on the
40 quality of the reporting. For some databases this number is included in a parameter of intensity or
41 size of each event. Typically, for large databases however, this is merely qualitative and describes
42 not only the number of individual landslides, but also an impact such as economic or human losses.
43 This classification is commonly based on press releases and is therefore heavily biased on the news
44 outlet reporting each event (e.g. Carrara et al., 2003).



45 Landslides triggered by catastrophic events, such as earthquakes or major storms, are often counted
46 as one event containing thousands of individual landslides (Kirschbaum et al., 2015). In contrast,
47 landslides caused by non-catastrophic events such as reasonable rainfall, are commonly counted as
48 individual events, disregarding their shared trigger. Consequently, the overall extent of clustering
49 in landslides is often unknown. But only if we better understand the extent of clustering between
50 individual landslide events, will we be able to understand the patterns they occur in and have the
51 chance to utilize these patterns to improve our forecast models (e.g. Martelloni et al., 2012).

52 Until now, few studies have focused on rainfall triggered landslide clusters and rather on temporal
53 clusters over a long time period within a confined region (e.g. Samia et al., 2017; Witt et al., 2010).
54 Biasutti et al. (2016) investigated the spatiotemporal clustering due to rainfall events for three
55 selected urban areas of the US West Coast: Seattle, San Francisco and Los Angeles. Over the nine
56 year study period, they found approximately 20 days within each city with multiple (up to eight)
57 landslide events. Additionally, they could identify close to 40 landslide events that were followed
58 by another event within the next week. However, with a focus on only selected study areas, they
59 did not show the overall extend of these clusters.

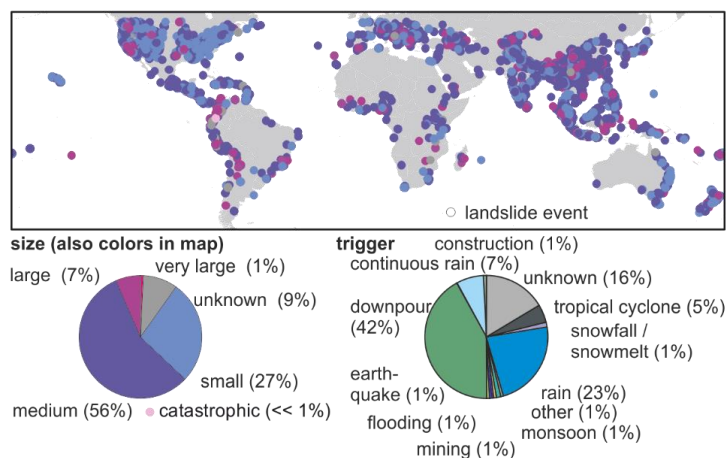
60 The objective of this study is therefore to develop an algorithm, which is able to identify such
61 clusters on a global scale. By applying the algorithm to the Global Landslide Catalog (GLC) the
62 overall degree of clustering in the database is shown, and spatial patterns of clusters with at least
63 10 landslide events are described. Additionally, landslide events and rainfall patterns of the most
64 intense and longest clusters are comprehensively discussed. In contrast to previous studies, such as
65 by Biasutti et al. (2016), clusters here are not constricted by a maximum spatial extent, instead they
66 are grouped by analyzing and comparing rainfall prior to the event at the event locations.



67 **2. Material and Method**

68 **2.1 Landslide Data**

69 All landslide events within this study are part of the Global Landslide Catalog (GLC) operated by
 70 NASA and introduced in Kirschbaum et al. (2010, 2015). Data within the catalogue is based on
 71 online news articles that are found through search engine options such as Google Alerts. In the
 72 presented study, only events with a location accuracy ≤ 25 km are considered. As the rainfall data
 73 used is only available within $\pm 50^\circ$ Latitude, landslide events outside of this range are not
 74 considered. Overall, a total of 9279 landslide events, ranging from 1988 to 2018 are analyzed (Fig.
 75 1). However, only 45 of these events occurred before 2007, when the GLC was established.



76
 77 **Figure 1.** Map of all landslide events analyzed in this study and their size (also color in map) and apparent trigger.
 78 Overall a total of 9279 events were tested for clustering.

79 For each event, the GLC provides a landslide type, e.g. land- or mudslide, and a landslide trigger,
 80 e.g. rainfall, downpour, earthquakes or construction work. Detailed descriptions on these
 81 classifications can be found in Kirschbaum et al. (2010, 2015). Furthermore, within the GLC the
 82 intensity, impact, and number of landslides per event is expressed in a variable called “size”. While
 83 events classified as small in the database are only a single landslide, medium or larger landslide



84 events may consist of multiple landslides within an unspecified range. About 64 % of the studied
85 events are classified as medium or larger in size. However, a precise count of the number of
86 landslides contained within these events does not exist in this database nor in any other of the global
87 scale databases currently available. Within the GLC most of the small events that contain only a
88 single landslide, are located within the United States (Fig. 1).

89 **2.2 Rainfall Data**

90 For the rainfall analysis, the Climate Hazards Group InfraRed Precipitation with Station data
91 (CHIRPS) (Climate Hazards Group, 2015) is used, which has a resolution of $0.05^\circ \times 0.05^\circ$ and
92 daily time steps. For each landslide event location, precipitation data were downloaded for 30 days
93 preceding the event and up to two days after the event using Google Earth Engine (Gorelick et al.,
94 2017). In order to compare rainfall during the event to overall rainfall at the location, the 95th
95 percentile of precipitation excluding non-rainy days was determined for 10 years prior to the event.
96 This comparison was also previously used by Kirschbaum et al (2015) to identify rainfall triggered
97 landslide events. However, in their case, rainfall data from the Tropical Rainfall Measuring Mission
98 (TRMM) was used for the time period 2000–2013 independent of the date of the landslide event.
99 Due to the higher spatial resolution CHIRPS data was used here instead.

100 In addition to the 95th percentile of rainfall, the global rainfall threshold by Guzzetti et al. (2008)
101 was also utilized to determine the likelihood of the individual landslide events being triggered by
102 rainfall. In their study 2626 rainfall events that have resulted in shallow landslides and debris flows
103 were analyzed in order to determine the following global rainfall intensity–duration threshold
104 [<http://rainfallthresholds.irpi.cnr.it>]:

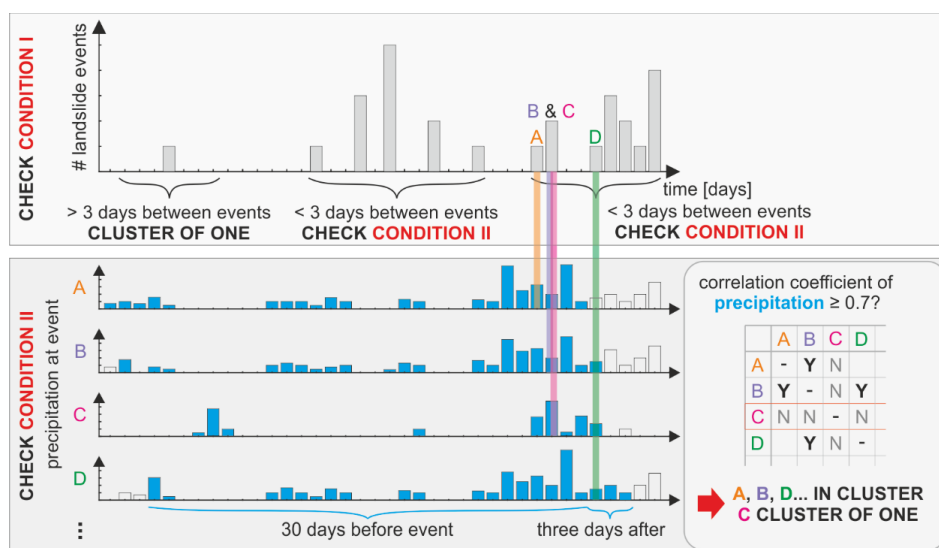
$$I = 2.2 \cdot D^{-0.44} \quad (1)$$



105 Here the threshold intensity (I) was determined for each 24 hours starting with a duration (D) of
106 12 hours. This results in an average precipitation of 0.73 mm/h for $D = 12$ h, 0.45 mm/h for $D =$
107 36 h, and 0.35 mm/h for $D = 60$ h. The rainfall threshold was then compared to the cumulative
108 mean precipitation of the rainfall event preceding each landslide event.

109 **2.3 Method**

110 The main objective of this study is to identify clusters of landslide events that occurred during, and
111 are likely triggered by the same rainfall event. To determine if two events, A and B, occurred during
112 the same rainfall event, two conditions have to be fulfilled: (I) A and B occurred within three days
113 of each other, and (II) spearman correlation between daily precipitation at A and at B is > 0.7 and
114 has a p-value < 0.05 for the 30 days preceding the later of the two events. Other landslide events
115 that fulfill these conditions with either A or B, are considered to be part of the cluster. A schematic
116 drawing of this algorithm is given in Fig. 2. The threshold value of three days maximum between
117 two events was used following Biasutti et al. (2016), who found it unlikely that landslide events
118 occurring more than three days apart, occurred during the same rainfall event. However, it is
119 important to note that their study was set in three metropolitan areas on the West Coast of the USA
120 and might not be applicable everywhere. The threshold value of the spearman correlation
121 coefficient was determined by testing the robustness of the identified clusters for different threshold
122 values between zero and one (Fig. S1). It was set to be 0.7 as from here on numbers of landslides
123 per cluster, duration of clusters, and area of clusters are stable for their mean and maximum values
124 (Fig. S1).



125

126 **Figure 2.** Schematic drawing of the algorithm used to identify, if two landslide events within the Global Landslide
 127 Catalog (GLC) occurred during the same rainfall event and hence belong to the same cluster. For condition II only
 128 events occurring within three days of each other are compared.

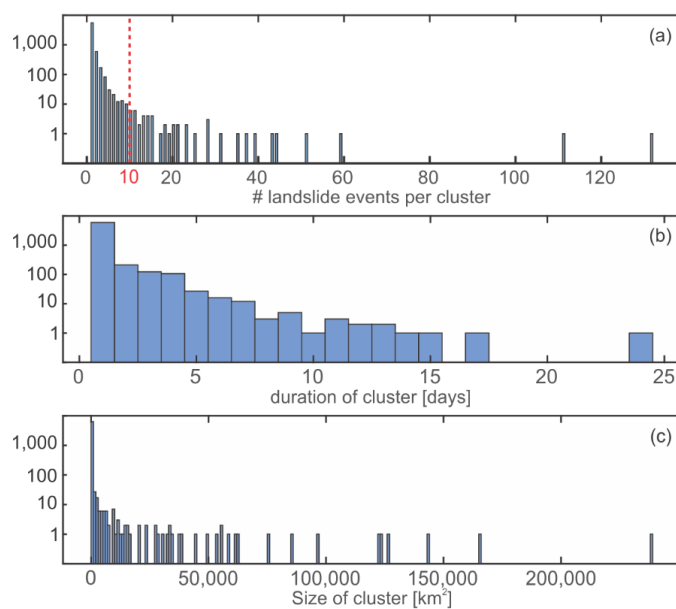
129 3. Results and Discussion

130 3.1 Clustering Characteristics

131 The presented algorithm divided the 9279 landslide events of the Global Landslide Catalog (GLC)
 132 into 6474 clusters of events connected through precipitation. However, 85 % of these clusters
 133 consist of only a single landslide event, containing in total 59 % of all recorded landslide events.
 134 This implies that a large number of landslide events are in fact isolated events with no association
 135 to other events. Nevertheless, 67 % of these ‘single landslide event’-clusters are categorized as
 136 medium or larger and might contain more than one landslide (in comparison 58 % of the landslide
 137 events in clusters \geq one landslide event are categorized as medium or larger). Hence, the number
 138 of isolated landslides is likely to be significantly smaller than the number of isolated landslide
 139 events.



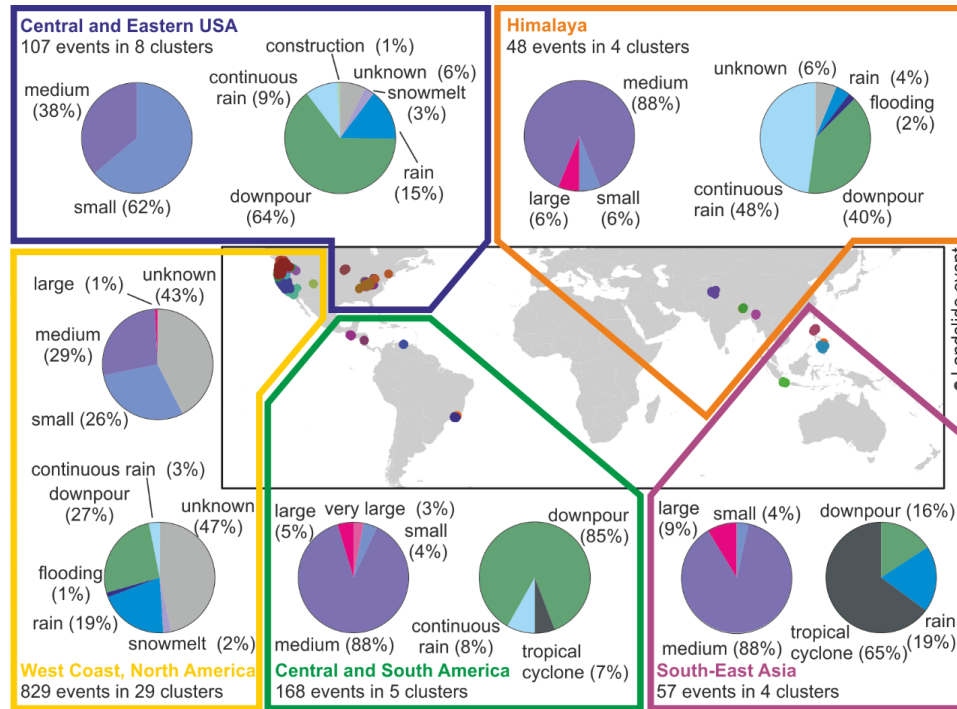
140 In the Global Landslide Catalog (GLC) only 3 % of the analyzed landslide events are linked to
141 triggers unrelated to rainfall such as construction, volcanos or earthquakes. This number is reduced
142 to 1.5 % for landslides in a cluster of more than one event. Due to the low number of events in this
143 category, future research is necessary to test and thoroughly validate these findings as well as to
144 assess possible reasons and implications of this phenomenon. For now, we assume that this is
145 mainly caused by biased reporting and cataloging of landslide events, where events linked to larger
146 disasters such as earthquakes, might be reported as one large landslide event, whereas landslides
147 linked to rainfall, might be individually reported. Similar observations were previously made by
148 Kirschbaum et al. (2015) for events in the GLC that are linked to major storms. An example of this
149 is the catastrophic magnitude 7.8 Gorkha earthquake in Nepal in 2015. While more than 25,000
150 landslides occurred during the earthquake and its aftershock sequence (e.g. Roback et al., 2018),
151 they are only reported as 13 landslide events in the excerpt from the GLC analyzed here. In it, they
152 are described as ranging in size from small to large and their trigger is given as “unknown”,
153 “earthquake” and in one case “snowmelt”. Our algorithm sorts these events into eight clusters of
154 up to three events.



155

156 **Figure 3.** Histogram of the number of events per cluster, duration of clusters and area of the convex hull of each cluster.
157 Clusters with only a single landslide event were appointed an area of zero. Within this study, all clusters with at least
158 10 landslide events were analyzed more closely.

159 Figure 3 provides histograms of the landslide events per cluster, duration of clusters and area
160 covered by clusters (convex hull) in a logarithmic scale. As expected, for all three aspects frequency
161 reduces drastically for larger numbers. In the following section all 50 clusters with at least 10 events
162 (marked in red in Figure 3) are evaluated more closely.



163

164 **Figure 4.** Location of all landslide events within clusters ≥ 10 events (different colors indicate different clusters).
 165 Overall, clusters in five distinct regions could be identified in the GLC (see Table S1 for more detail). Size and trigger
 166 (GLC categorization) of the associated landslide events are also shown.

167 3.2 Clusters with more than ten Landslide Events

168 3.2.1 Global Analysis

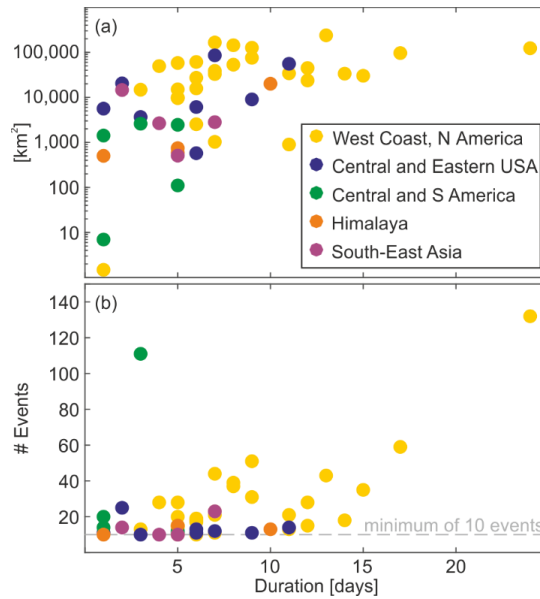
169 Table S1 gives more detail of the 50 clusters with at least 10 events. In total 13 % of all landslide
 170 events are associated with one of these clusters. As the database is most likely incomplete, the true
 171 number is expected to be higher. Overall the algorithm detects clusters in five distinct regions: (1)
 172 West Coast of North America, (2) Central and Eastern USA, (3) Central and Southern America, (4)
 173 Himalaya Region and (5) South-East Asia (Fig. 4). However, close to three quarters of all clusters
 174 ≥ 10 events are found within the USA mostly due to a bias in the GLC database (Kirschbaum et
 175 al., 2015) (Fig. 1). This is also shown in the size of recorded landslide events (Fig. 4).



176 In North America events are often classified as small in size, while clusters in the other regions
177 contain mainly medium events. This might be due to English speaking media, on which the GLC
178 is based, only picking up on large international events that consist of multiple landslides within an
179 area and smaller ones are under or not reported at all.

180 The median clusters with at least 10 events last six days, consist of 15 events, and span over an
181 area of 15,000 km² (Fig. 5). As expected, there is a positive correlation between cluster duration
182 and area (spearman correlation coefficient of 0.70, p-value: 0.001). However, this cannot be
183 observed for cluster duration and number of landslide events within the cluster (spearman
184 correlation coefficient of 0.44, p-value: 0.001). When comparing the different regions, clusters
185 located on the West Coast of North America are on average the longest and cover the largest area.
186 In contrast, events in South America are shortest and smallest, nevertheless they have the highest
187 number of events and clusters per day (Table 1).

188 On a global scale, no significant trend over time can be observed and clusters with ≥ 10 events
189 occur around the year (Fig. S2). Similarly, the total number of reported landslide shows no
190 significant increase in the GLC (Kirschbaum et al., 2015) as well as in other global databases such
191 as the Global Fatal Landslide Database (Froude and Petley, 2018). More regional observations
192 show seasonal variation and are described more closely in the following chapters. However, for
193 three out of the five regions, there are only five clusters or even less.



194

195 **Figure 5.** Link between the duration of the individual clusters ≥ 10 events and a) the covered area and b) the number
 196 of landslide events per cluster. The color of the scatter plots indicates the region, in which each cluster occurred.

197 **Table 1.** Regional statistics for all landslide clusters (LC) with at least ten landslide events (LE).

| Region | # LC | # LE | LE per LC | Average duration of LCs | LEs per day | Average area of LCs [km ²] | Percentage of LE in a LC ≥ 10 LE |
|---------------------------|------|------|-----------|-------------------------|-------------|--|---------------------------------------|
| West Coast, North America | 29 | 829 | 28.6 | 9 | 3.3 | 52,970 | 31 |
| Central and Eastern USA | 8 | 107 | 13.4 | 6 | 2.4 | 23,357 | 12 |
| South and Central America | 5 | 168 | 33.6 | 3 | 11.2 | 1,320 | 18 |
| Himalaya | 4 | 48 | 12.0 | 5 | 2.3 | 5,476 | 3 |
| South-East Asia | 4 | 57 | 14.3 | 5 | 3.2 | 5,143 | 4 |

198

199 3.2.2 West Coast, North America

200 Landslides in the west of North America have been intensively investigated, mainly in the form of
 201 case studies that discuss landslides along the Pacific coast in the states of California (Collins and
 202 Sitar, 2008; Wieczorek, 1988), Oregon (Benda, 1990; Miller and Burnett, 2008) and Washington



203 (LaHusen et al., 2016; Perkins et al., 2017). This region is also one of the few, where the clustering
204 of rainfall triggered landslide events was previously investigated, showing qualitatively that there
205 are many instances in which landslides occur on consecutive days (Biasutti et al., 2016).

206 About 31 % of all landslide events recorded in this area belong to a cluster of at least ten events.
207 This is the highest number compared to the other regions of the world (Table 1). However, this
208 effect might be amplified by the high number of reported landslides. The large number of events
209 and clusters is mainly due to geologic, topographic, climatic conditions and construction practices.
210 For example in Oregon, steep slopes and heavy rainfalls are as well as poor construction practices
211 result in high economic losses (Wang et al., 2002). Burns et al. (2017) estimated an average annual
212 loss of \$15.4 million due to landslides in Oregon alone. In years with heavy storms such as 1996,
213 this can accumulate to more than \$100 million (Wang et al., 2002).

214 The observed clusters in this area are among the longest and have the largest areas of all regions
215 (Table 1). While the size of landslide events (as given by the GLC) in the west of North America
216 are small compared to most other regions, there is also a considerable amount of events, where the
217 size is unknown (43 %, Fig. 4). While about half of the landslide events within clusters ≥ 10 events
218 are classified as “trigger unknown” (47 %), landslide events with a known cause are mainly
219 triggered by downpour (27 %) or rain (19 %) (Fig. 4). However, when looking at satellite based
220 rainfall data preceding the clusters, rainfall cannot always be identified as a trigger (Fig. S3). While
221 it generally exceeds the global rainfall threshold (Guzzetti et al., 2008), the 95th percentile of
222 precipitation on rainy days is not reached for the majority of the clusters. Although, several studies
223 linked landslides within California to earthquakes (e.g. Harp and Jibson, 1996; Keefer, 2000), they
224 occurred before 2007 and are not registered in the GLC.



225 While there appears to be no significant change in the number of clusters over time (Fig. S2), most
226 clusters occur during the rainy season (November to March), when most landslide events occur.
227 Within the west of North America this time period is therefore often referred to as the “landslide
228 season” (e.g. Mirus et al., 2018). Only one cluster in this region appears in June (Cluster ID 21,
229 Table S1). However, the center of this cluster is located more inland (in San Miguel County,
230 Colorado) and is also the shortest cluster (only one day) within the region as well as the most local
231 of all clusters in this study, covering only 1 km². While this cluster is triggered by downpour
232 according to the GLC, this is not apparent from satellite derived precipitation (Fig. S3). The small
233 size of the cluster might be the reason, why low-resolution satellite derived precipitation does not
234 record any anomalies here.

235 **3.2.3 Central and Eastern USA**

236 While most of the clusters with ≥ 10 landslides events of this region, are located in the Appalachian
237 Plateau (Ohio, West Virginia and Kentucky), one cluster can be found in Minnesota (ID 34 in Table
238 S1 and Fig. S4). While it is considerably smaller (580 km² compared to $> 9,000$ km²), it is
239 comparable to the Appalachians cluster in its number of landslide events and duration. The
240 Appalachian Plateau is well known for its landslides and the annual direct cost in Kentucky exceeds
241 \$10 million (Crawford and Bryson, 2017).

242 Like the landslide clusters observed in the west of North America, clusters here consist mainly of
243 small landslides, which is most likely linked to the news alerts on which the GLC is based.
244 Checking sources in the GLC, they are mainly reported within smaller, more local news outlets
245 compared to landslide events outside of the US. To our knowledge the individual events grouped
246 by our algorithm into clusters have never been linked before. Clusters in this region occur
247 predominantly in spring (February to June), when rainfall is highest, slightly later than events on



248 the West Coast (Fig. S2). According to GLC they are predominantly triggered by downpours (64 %,
249 Fig. 4). However, extreme rainfall is not always visible in satellite derived precipitation (Fig. S4).
250 For most clusters, it is below the 95th percentile, but above the global threshold. It is worth noting
251 than one cluster located in West Virginia (Cluster ID 35) shows no rainfall on the satellite before
252 day three of the cluster. Following the GLC, early landslide events within this cluster are linked to
253 snowmelt.

254 **3.2.4 Central and South America**

255 In contrast to the clusters in North America, more than 95 % of landslide events within clusters of
256 this region are medium in size or larger and might consists of several landslides themselves (Fig.
257 4). Thus, the number of landslides per cluster and per day is likely to be significantly higher than
258 the number of events per cluster and per day. Still, clusters in this area are on average only two and
259 a half days long, covering an area of slightly over 1,500 km² and they are the smallest and shortest
260 of all regions (Fig. 5, Table 1). It is important to note that this region covers the largest area reaching
261 from Rio de Janeiro in Brazil to Guatemala in Central America. From the few clusters we could
262 identify, it appears that there are dissimilarities between the clusters in Central America and South
263 America. The two clusters in Nicaragua (ID 42) and Guatemala (ID 39) are triggered by continuous
264 rain and a tropical cyclone, respectively. In contrast, all events located in South America (IDs 38,
265 40, and 41) are all triggered by downpour (Table S1 and Fig. S5).

266 **3.2.5 Himalaya**

267 Like in South America, most landslide events (94 %) associated with clusters with ≥ 10 events in
268 the Himalaya region are categorized as medium and larger. Thus, the number of landslides per
269 cluster is again expected to be significantly higher than the number of landslide events per cluster.
270 However, there may be differences between regions. Event ID 44, located in India and Pakistan



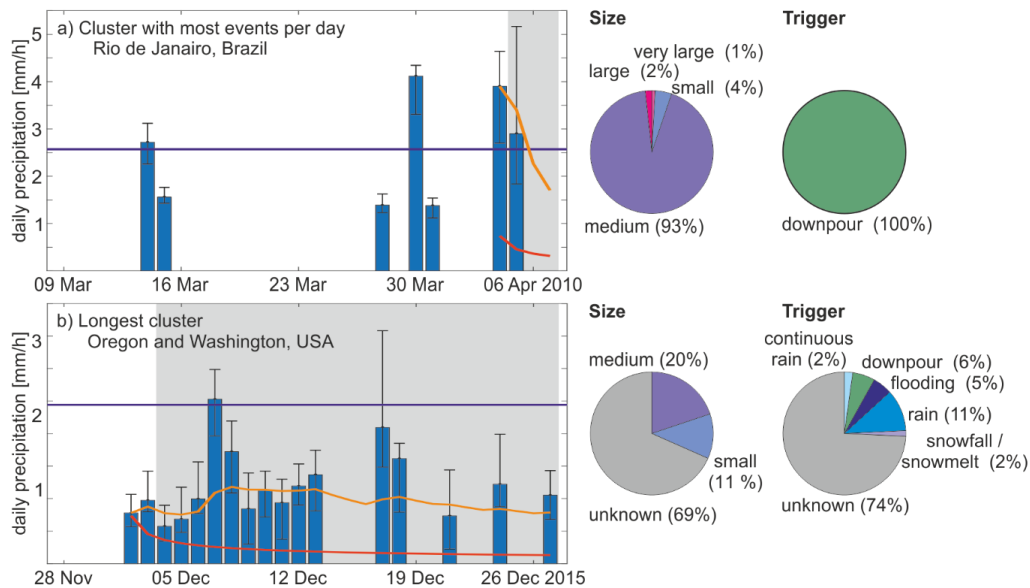
271 around Jammu and Kashmir, is classified as medium to small, much longer (10 days) and covers
272 an area more than 10 times larger than the other clusters. All of them are classified as medium or
273 large and are located in the East of India with some events in Nepal (Table S1). In both regions,
274 clusters are triggered by continuous rain or downpour. For all clusters satellite based rainfall data
275 exceeds the global threshold, and in most cases the 95th percentile of rainfall on rainy days (Fig.
276 S6). It is important to note that while earthquake triggered landslides are common in the region
277 (e.g. Parkash, 2013; Roback et al., 2018), the presented algorithm is by design only able to pick up
278 clusters that are linked by rainfall.

279 **3.2.6 South-East Asia**

280 As only four clusters are identified in this region, a detailed analysis is impossible. Again, 96 % of
281 the events associated are categorized as medium or larger and the main triggers are tropical
282 cyclones (Cluster IDs 47 and 48), downpour (Cluster ID 49), and rain (ID 50) (Table S1). Here,
283 satellite based rainfall data before clusters is both above the global rainfall threshold and in most
284 cases above the 95th percentile (Fig. S7). While only one of the four clusters (ID 50) is recorded
285 outside of the Philippines (in Indonesia), there is no apparent difference between both countries
286 (Table 1).

287 **3.3 Most Intense Cluster**

288 The cluster with the most events in one day, i.e. most intense cluster, happened in Rio de Janeiro,
289 Brazil, as well as neighboring cities Niteroi and Sao Goncalo in 2010. In an area of approximately
290 2,800 km², 111 landslide events were recorded within only three days, however predominantly on
291 6th April 2010 (Table S1, ID 38). This is almost four times as many landslide events in a single day
292 than the second most intense clusters (IDs 1 and 3) located in Washington and Oregon, USA. Both
293 recorded 29 events in one day.



294

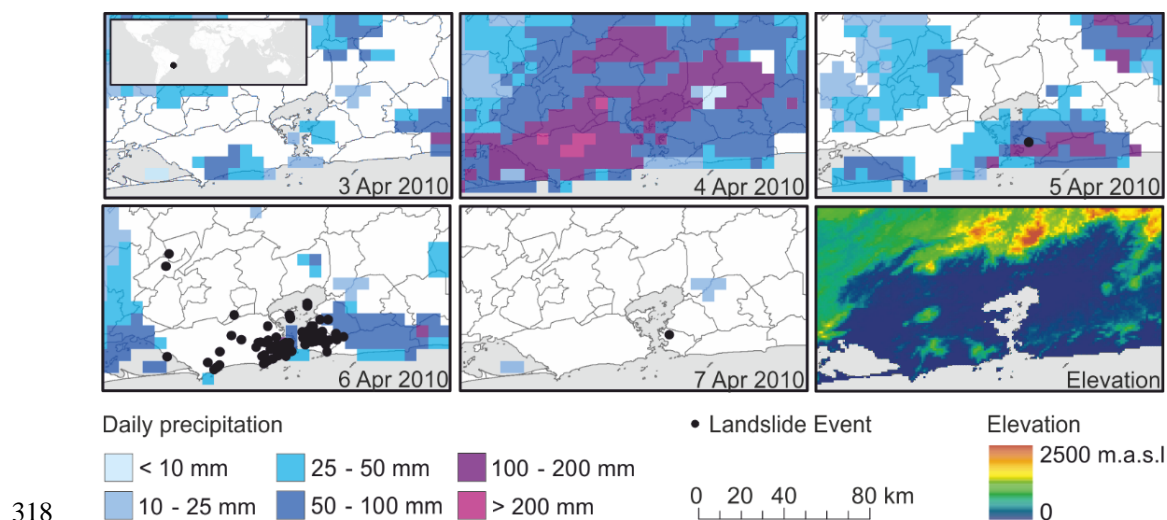
295 **Figure 6.** Daily precipitation for 30 days preceding the last landslide event of the cluster with the size of the associated
 296 landslide events and their trigger according to the GLC. Shown is the median precipitation for all landslide locations
 297 with the inner quartiles as an error bar. The 95th percentile of daily rainfall (rainy days only) in the ten years preceding
 298 the event is given in blue, in red the global rainfall threshold ID (Guzzetti et al., 2008) and in orange the cumulative
 299 mean for the rainfall event preceding the cluster. a) Cluster with the most events per day (ID 43), and b) longest running
 300 cluster (ID 22).

301 Most of the 111 events associated with the cluster in Rio de Janeiro were recorded as medium in
 302 size, all of which were triggered by downpour (Fig. 6a). This is confirmed by satellite derived
 303 precipitation. Heavy rainfalls (Figs. 6a, 7) occurred on the 4th and 5th of April of up to 210 mm per
 304 day. In comparison, the 95th percentile in the 10 years preceding this cluster is on average only 62
 305 mm per day (rainfall for each individual location shown in Fig. S8). While the rainfall covered a
 306 large area, landslide events were primarily reported for steep slopes just outside the densely
 307 populated city center. Due to its location close to, and inside the urban area of Rio de Janeiro, the
 308 cluster caused approximately 200 fatalities according to CNN news reports
 309 (<http://www.cnn.com/2010/WORLD/americas/04/12/brazil.flooding.mudslides/>).



310 The location in the city might also be the reason for the large number of events being reported, as
311 we can expect more individual landslides being reported here compared to the countryside.

312 While studies not based on English speaking news alerts report a large number of landslides within
313 and around Rio de Janeiro (Calvello et al., 2015; Sandholz et al., 2018), only nine additional
314 landslide events inside the area of this cluster were reported in the GLC between 2009 and 2018.
315 Additionally, just northwest of the cluster another cluster occurred in January 2011 (ID 41 in Table
316 S1, Fig. S5). Although, this cluster only counts 20 individual landslide events within the GLC, it
317 is being reported as thousands individual landslides (Coelho Netto et al., 2013).



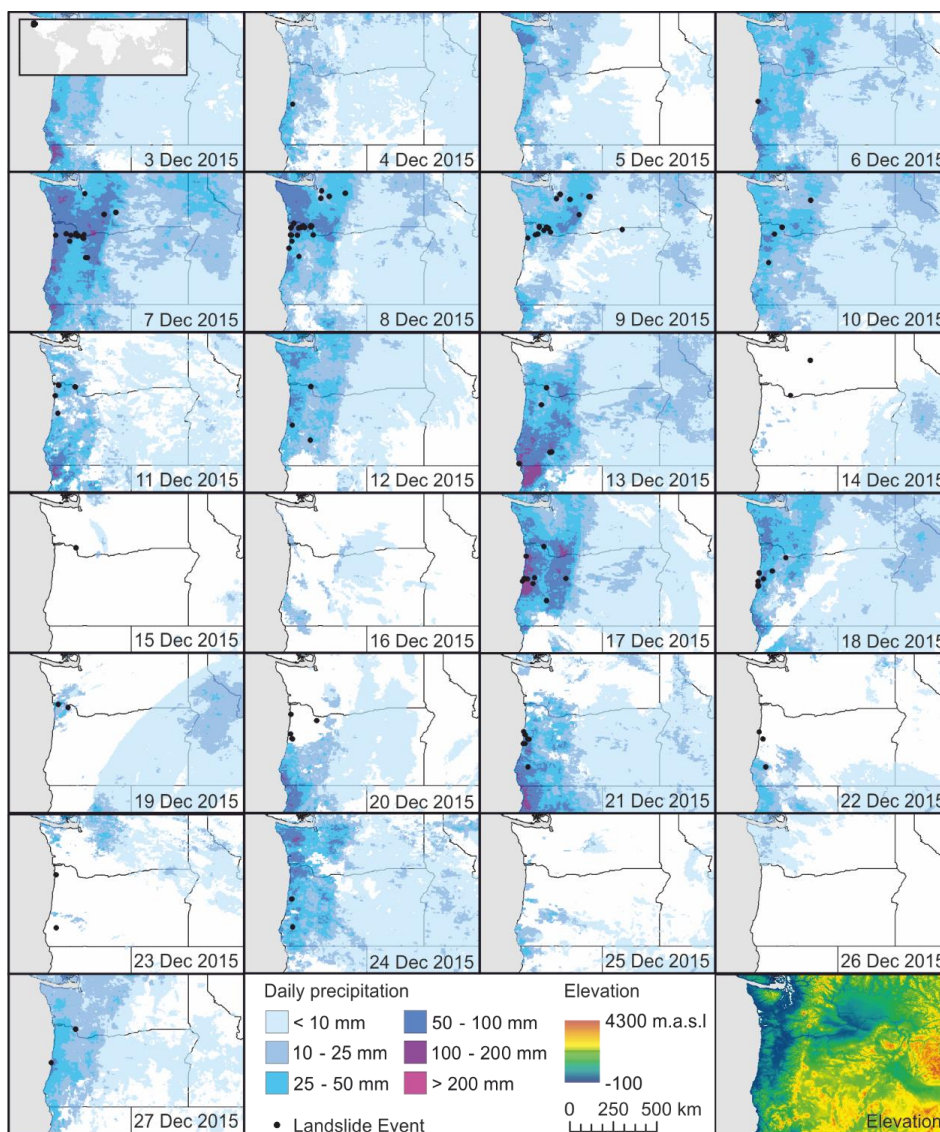
318 **Figure 7.** Location of the events in the cluster with the most events per day located in Rio de Janeiro, Brazil. Also
319 shown are daily precipitation and elevation. Elevation data is taken from the US Geological Survey (GTOPO30).
320

321 **3.4 Longest Cluster**

322 The longest running cluster identified in this study occurred in Oregon and Washington, USA from
323 4th to 27th December 2015 for a total of 24 days with 132 landslide events (Cluster ID 18, Table
324 S1). The second longest cluster lasted 17 days over January and February in 2012 and was also



325 located in Oregon and Washington, USA (Cluster ID 7). Overall, most events within the longest
326 cluster are unknown in size (69 %) and trigger (74 %) (Fig. 6b). However, inspecting satellite based
327 rainfall data, continuous rainfall appears to be the main trigger (Fig. 6b, Fig. 8 and Fig. S9 for
328 rainfall at the individual event locations). While daily rainfall is mainly below the 95th percentile,
329 cumulative mean rainfall is continuously above the global rainfall threshold. Although, heavy
330 rainfall is common in this area during winter times, for this cluster it lasted longer than usual and
331 was followed by shorter rain events in short successions (Fig. 8). Thus, the series of landslides did
332 not halt resulting in the longest cluster in the GLC. Following the information on sources within
333 the GLC, it appears that local media reported about the individual landslide events, but did not
334 detect on the extreme length of the continuous series of landslide events at this point in time (e.g.
335 <https://kval.com/news/local/landslide-blocks-i-5-in-sw-washington;>
336 [https://q13fox.com/2015/12/09/landslide-above-puget-sound-damages-several-homes-at-least-](https://q13fox.com/2015/12/09/landslide-above-puget-sound-damages-several-homes-at-least-one-vehicle/)
337 [one-vehicle/](https://q13fox.com/2015/12/09/landslide-above-puget-sound-damages-several-homes-at-least-one-vehicle/)). As landslide events are such a common occurrence in this region, and due to the
338 large area covered by this cluster, there is currently little to no emphasis on the longevity of this
339 specific series of landslide events in media and scientific studies.



341

342 **Figure 8.** Location and time series of the longest cluster, located mainly in Oregon, USA. Also shown are daily rainfall
343 and elevation. Elevation data is available from the US Geological Survey (GTOPO30).

344 4. Conclusion

345 In this study an algorithm is presented that detects clusters of landslide events that occur during,
and are likely triggered by the same rainfall events. Here this algorithm is applied to the Global



346 Landslide Catalog (GLC), where it detects that more than 40 % of all recorded events can be linked
347 to at least one other event. The global analysis shows that 14 % of all landslide events are part of a
348 cluster ≥ 10 events. However, this percentage varies dramatically by the region, ranging from 30 %
349 on the West Coast of North America to 3 % in the Himalayas. Part of this is caused by sampling
350 and reporting bias. As the GLC is based on English speaking media, events in the USA are reported
351 and cataloged in much greater detail than events abroad. Nevertheless, within the GLC we could
352 detect clusters ≥ 10 landslide events in five distinct regions: (1) West Coast of North America, (2)
353 Central and Eastern USA, (3) Central and Southern America, (4) Himalaya Region, and (5) South-
354 East Asia. In South America, the studied clusters are the shortest, but contain the most events per
355 day. However, this is mainly due to a cluster in Rio de Janeiro, where 108 of events were recorded
356 on 6th April 2010. As most of these events are classified as medium or larger, the absolute number
357 of landslides is expected to be significantly higher. In contrast, the longest and largest clusters are
358 observed on the West Coast of North America. On average clusters here last nine days and cover
359 an area of more than 50,000 km². The steep slopes and continuous rainfalls present in the area
360 combined with the above average reporting of landslide events, makes a more detailed analysis of
361 rainfall related landslide clusters possible. The longest of all detected clusters ≥ 10 landslide events
362 is also located in this region: In December 2015, 132 landslide events were recorded over a time
363 period of 24 days spanning more than 120 thousand km², which were all triggered by the same
364 rainfall event. Detection of large scale clusters such as this one can not only help to improve our
365 understanding of the link between individual events, but also be used in our mitigation strategies.
366 Only once we improve our understanding of the relation between individual landslide events, we
367 will be able to predict their behavior and forecast their economic losses and fatalities. While our
368 study does not replace case specific and small scale studies, as well as the identification of threshold
369 values, it can provide an improved understanding for managing landslide mitigations on a larger



370 scale. Within the area covered by individual clusters the same mitigation strategies, including early
371 warning systems (EWS) based on weather forecast simulations, can be developed and validated.
372 For future research we recommend to use the presented algorithm not only for the correlation with
373 precipitation data, but also to include the geometry of atmospheric rivers during cluster detection.
374 Finally, the algorithm could be applied to more regional and other global landslide databases
375 thereby improving our understanding on the spatial and temporal occurrence of landslide clusters.

376 **References**

377 Benda, L.: The influence of debris flows on channels and valley floors in the Oregon Coast Range,
378 U.S.A., *Earth Surface Processes and Landforms*, 15(5), 457–466, doi:10.1002/esp.3290150508,
379 1990.

380 Biasutti, M., Seager, R. and Kirschbaum, D. B.: Landslides in West Coast metropolitan areas: The
381 role of extreme weather events, *Weather and Climate Extremes*, 14, 67–79,
382 doi:10.1016/j.wace.2016.11.004, 2016.

383 Burns, W. J., Calhoun, N. C., Franczyk, J. J., Koss, E. J. and Bordal, M. G.: Estimating losses from
384 landslides in Oregon, Roanoke, VA., 2017.

385 Calvello, M., d’Orsi, R. N., Piciullo, L., Paes, N., Magalhaes, M. and Lacerda, W. A.: The Rio de
386 Janeiro early warning system for rainfall-induced landslides: Analysis of performance for the years
387 2010–2013, *International Journal of Disaster Risk Reduction*, 12, 3–15,
388 doi:10.1016/j.ijdr.2014.10.005, 2015.

389 Carrara, A., Crosta, G., and Frattini, P.: Geomorphological and historical data in assessing landslide
390 hazard, *Earth Surf. Proc. Land.*, 28, 1125–1142, <https://doi.org/10.1002/esp.545>, 2003.

391 Climate Hazards Group: CHIRPSv2.0, , doi:10.15780/G2RP4Q, 2015.



- 392 Coelho Netto, A. L., Sato, A. M., de Souza Avelar, A., Vianna, L. G. G., Araújo, I. S., Ferreira, D.
393 L. C., Lima, P. H., Silva, A. P. A. and Silva, R. P.: January 2011: The Extreme Landslide Disaster
394 in Brazil, in *Landslide Science and Practice*, edited by C. Margottini, P. Canuti, and K. Sassa, pp.
395 377–384, Springer Berlin Heidelberg, Berlin, Heidelberg., 2013.
- 396 Collins, B. D. and Sitar, N.: Processes of coastal bluff erosion in weakly lithified sands, Pacifica,
397 California, USA, *Geomorphology*, 97(3), 483–501, doi:10.1016/j.geomorph.2007.09.004, 2008.
- 398 Crawford, M. and Bryson, L.: Field Investigation of an Active Landslide In Kentucky: A
399 Framework to Correlate Electrical Data and Shear Strength, Kentucky Geological Survey Report
400 of Investigations, doi:<https://doi.org/10.13023/kgs.ri01.13>, 2017.
- 401 Froude, M. J. and Petley, D. N.: Global fatal landslide occurrence from 2004 to 2016, *Natural*
402 *Hazards and Earth System Sciences*, 18(8), 2161–2181, doi:10.5194/nhess-18-2161-2018, 2018.
- 403 GLC: Global Landslide Catalog, NASA’s Open Data Portal [online] Available from:
404 [https://data.nasa.gov/d/h9d8-neg4?category=Earth-Science&view_name=Global-Landslide-](https://data.nasa.gov/d/h9d8-neg4?category=Earth-Science&view_name=Global-Landslide-Catalog)
405 *Catalog* (Accessed 3 May 2018), n.d.
- 406 Gorelick, N., Hancher, M., Dixon, M., Ilyushchenko, S., Thau, D. and Moore, R.: Google Earth
407 Engine: Planetary-scale geospatial analysis for everyone, *Remote Sensing of Environment*, 202,
408 18–27, doi:10.1016/j.rse.2017.06.031, 2017.
- 409 Guzzetti, F., Peruccacci, S., Rossi, M. and Stark, C. P.: The rainfall intensity–duration control of
410 shallow landslides and debris flows: an update, *Landslides*, 5(1), 3–17, doi:10.1007/s10346-007-
411 0112-1, 2008.
- 412 Guha S, Below R, Ph. Hoyois Ph (2015) EM-DAT: International Disaster Database –
413 www.emdat.be – Université Catholique de Louvain – Brussels – Belgium



- 414 Harp, E. L. and Jibson, R. W.: Landslides triggered by the 1994 Northridge, California, earthquake,
415 Bulletin of the Seismological Society of America, 86(1B), S319–S332, 1996.
- 416 Keefer, D. K.: Statistical analysis of an earthquake-induced landslide distribution — the 1989
417 Loma Prieta, California event, Engineering Geology, 58(3), 231–249, doi:10.1016/S0013-
418 7952(00)00037-5, 2000.
- 419 Kirschbaum, D. and Stanley, T.: Satellite-Based Assessment of Rainfall-Triggered Landslide
420 Hazard for Situational Awareness, Earth’s Future, 6(3), 505–523, doi:10.1002/2017EF000715,
421 2018.
- 422 Kirschbaum, D., Stanley, T. and Zhou, Y.: Spatial and temporal analysis of a global landslide
423 catalog, Geomorphology, 249, 4–15, doi:10.1016/j.geomorph.2015.03.016, 2015.
- 424 Kirschbaum, D. B., Adler, R., Hong, Y., Hill, S. and Lerner-Lam, A.: A global landslide catalog
425 for hazard applications: method, results, and limitations, Natural Hazards, 52(3), 561–575,
426 doi:10.1007/s11069-009-9401-4, 2010.
- 427 LaHusen, S. R., Duvall, A. R., Booth, A. M. and Montgomery, D. R.: Surface roughness dating of
428 long-runout landslides near Oso, Washington (USA), reveals persistent postglacial hillslope
429 instability, Geology, 44(2), 111–114, doi:10.1130/G37267.1, 2016.
- 430 Malamud, B. D., Turcotte, D. L., Guzzetti, F. and Reichenbach, P.: Landslide inventories and their
431 statistical properties, Earth Surface Processes and Landforms, 29(6), 687–711,
432 doi:10.1002/esp.1064, 2004.
- 433 Martelloni, G, Segoni, S., Fanti, R. and Catani, F.: Rainfall thresholds for the forecasting of
434 landslide occurrence at regional scale. Landslides, 9(4), 485–495, doi:10.1007/s10346-011-0308-
435 2, 2012.



- 436 Miller, D. J. and Burnett, K. M.: A probabilistic model of debris-flow delivery to stream channels,
437 demonstrated for the Coast Range of Oregon, USA, *Geomorphology*, 94(1), 184–205,
438 doi:10.1016/j.geomorph.2007.05.009, 2008.
- 439 Mirus, B., Morphew, M. and Smith, J.: Developing Hydro-Meteorological Thresholds for Shallow
440 Landslide Initiation and Early Warning, *Water*, 10(9), 1274, doi:10.3390/w10091274, 2018.
- 441 Parkash, S.: Earthquake Related Landslides in the Indian Himalaya: Experiences from the Past and
442 Implications for the Future, in *Landslide Science and Practice: Volume 5: Complex Environment*,
443 edited by C. Margottini, P. Canuti, and K. Sassa, pp. 327–334, Springer Berlin Heidelberg, Berlin,
444 Heidelberg., 2013.
- 445 Perkins, J. P., Reid, M. E. and Schmidt, K. M.: Control of landslide volume and hazard by glacial
446 stratigraphic architecture, northwest Washington State, USA, *Geology*, 45(12), 1139–1142,
447 doi:10.1130/G39691.1, 2017.
- 448 Petley, D.: Global patterns of loss of life from landslides, *Geology*, 40(10), 927–930,
449 doi:10.1130/G33217.1, 2012.
- 450 Roback, K., Clark, M. K., West, A. J., Zekkos, D., Li, G., Gallen, S. F., Chamlagain, D. and Godt,
451 J. W.: The size, distribution, and mobility of landslides caused by the 2015 M w 7.8 Gorkha
452 earthquake, Nepal, *Geomorphology*, 301, 121–138, doi:10.1016/j.geomorph.2017.01.030, 2018.
- 453 Samia, J., Temme, A., Bregt, A., Wallinga, J., Guzzetti, F., Ardizzone, F. and Rossi, M.: Do
454 landslides follow landslides? Insights in path dependency from a multi-temporal landslide
455 inventory, *Landslides*, 14(2), 547–558, doi:10.1007/s10346-016-0739-x, 2017.



456 Sandholz, S., Lange, W. and Nehren, U.: Governing green change: Ecosystem-based measures for
457 reducing landslide risk in Rio de Janeiro, *International Journal of Disaster Risk Reduction*, 32, 75–
458 86, doi:10.1016/j.ijdr.2018.01.020, 2018.

459 Wang, Y., Summers, R. D. and Hofmeister, R. J.: Landslide loss estimation - Pilot project in
460 Oregon, Oregon Department of Geology and Mineral Industries (DOGAMI), 2002.

461 Wieczorek, G. F.: Landslides, Floods, and Marine Effects of the Storm of January 3-5, 1982, in the
462 San Francisco Bay Region, California, USGS Numbered Series, Geological Survey (U.S.). [online]
463 Available from: <http://pubs.er.usgs.gov/publication/pp1434> (Accessed 6 November 2018), 1988.

464 Witt, A., Malamud, B. D., Rossi, M., Guzzetti, F. and Peruccacci, S.: Temporal correlations and
465 clustering of landslides, *Earth Surface Processes and Landforms*, 35(10), 1138–1156,
466 doi:10.1002/esp.1998, 2010.

467